JACS
JOURNAL OF THE AMERICAN CHEMICAL SOCIETY
pubs.acs.org/JACS
Article

# Ene Reactivity of an Fe=NR Bond Enables the Catalytic α-Deuteration of Nitriles and Alkynes

Yafei Gao, Maren Pink, Veronica Carta, and Jeremy M. Smith*

Cite This: J. Am. Chem. Soc. 2022, 144, 17165−17172
Read Online
ACCESS | Metrics & More | Article Recommendations | Supporting Information

**ABSTRACT:** Herein, we report the reactions of an Fe(II) imido complex $[Ph_2B(^tBuIm)_2Fe{=}NDipp]^-$ (**1**) with internal alkynes and isobutyronitrile, affording the Fe amido allenyl complexes $[Ph_2B(^tBuIm)_2Fe(NHDipp)((R_1)C{=}C{=}C(R_2)(H))]^-$ ($R_1$ = Et or $^n$Pr; $R_2$ = Me or Et, **2**−**5**) and the Fe amido keteniminate complex $[Ph_2B(^tBuIm)_2Fe(NHDipp)(N{=}C{=}CMe_2)K(THF)]_n$ (**8-K**), respectively. These transformations represent the previously unknown ene-like reactivity of a metal−ligand multiple bond. Stoichiometric reactions of **2** and **8-K** with $DippNH_2$ lead to the regeneration of 3-hexyne and isobutyronitrile, respectively, with concomitant formation of the bis(anilido) complex $[Ph_2B(^tBuIm)_2Fe(NHDipp)_2]^-$ (**9**). These results provide the platform for **1** as an efficient catalyst for the selective α-deuteration of nitriles and alkynes by $RND_2$. These results demonstrate a new reaction mode for metal imido complexes and suggest new avenues for using the imido ligand in catalysis.

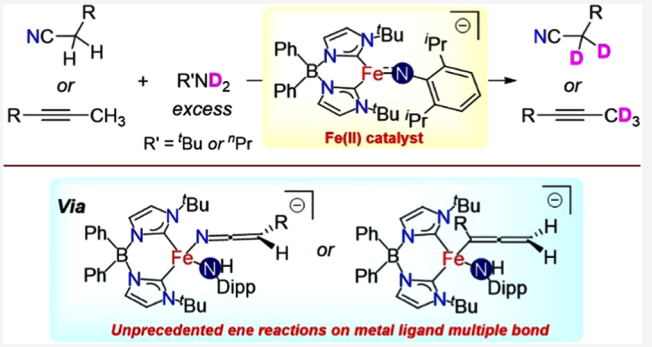


## INTRODUCTION

The ene reaction is a powerful method for constructing carbon−carbon and carbon−heteroatom bonds, with many applications in the synthesis of complex organic molecules.[1−6] The prototypical ene reaction occurs between an alkene containing allylic hydrogen (ene) and a multiple bond (enophile), leading to the formation of a new σ-bond concomitant with double-bond migration and a 1,5-hydrogen shift (Scheme 1(1)).[7] The ene reaction is not limited to alkenes, and unsaturated functionalities such as alkynes and allenes may also serve as ene substrates.[8] The uncatalyzed ene reaction typically requires high temperatures;[9] however, certain Lewis acids have been shown to catalyze these transformations.[10,11]

While not normally considered in this context, in principle, transition-metal imido (M=NR) complexes could be considered as enophiles in ene reactions. However, the reactions of imido complexes with ene substrates commonly involve N-group transfer.[12−28] For example, internal alkynes and nitriles undergo [2 + 2] reactions with M=NR bonds to afford four-membered metallacycle intermediates (Scheme 1(2a)) that lead to nitrene transfer.[29−31] However, since the properties of the M=NR unit can be tailored through changes to the ancillary ligands,[32−34] suitable molecular design may allow imido complexes to be developed as enophiles. This would provide an opportunity to develop unusual metal-catalyzed transformations. However, to the best of our knowledge, ene reactions of metal imido complexes have never been proposed or observed.

We previously reported a three-coordinate Fe(II) imido complex $[Ph_2B(^tBuIm)_2Fe{=}NDipp]^-$ (**1**),[35] in which the degree of iron nitrogen π-bonding is attenuated by the high-spin ($S$ = 2) Fe center. Consequently, the nitrogen donor of the imido ligand is more basic/nucleophilic than in most late metal imido complexes. In addition, the basicity and reactivity of the imido ligand can be modulated by alkali metal ion coordination.[36] The enhanced basicity enables the catalytic guanylation of carbodiimides, a reaction that is more commonly associated with early metal imido complexes.[27] We reasoned that this enhanced basicity might redirect the reactivity of the imido ligand away from [2 + 2] reactions with unsaturated substrates, leading to new transformations.

In this manuscript, we report on the unusual reactivity of alkynes with **1**. While a terminal alkyne reacts to afford an amido acetylide complex, internal alkynes bearing α-C−H groups provide amido allenyl complexes. Similarly, isobutyronitrile reacts with **1** to afford an amido keteniminate complex. These reactions can be considered as ene reactions involving the Fe=NR unit (Scheme 1(2b)), which are without precedent in metal−ligand multiple bond chemistry. These

Received: July 14, 2022
Published: September 7, 2022

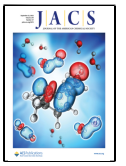







https://doi.org/10.1021/jacs.2c07462
J. Am. Chem. Soc. 2022, 144, 17165−17172

**Scheme 1. Classical Ene Reactions and the Reactions of Transition-Metal Imido Complexes with Alkynes and Nitriles**

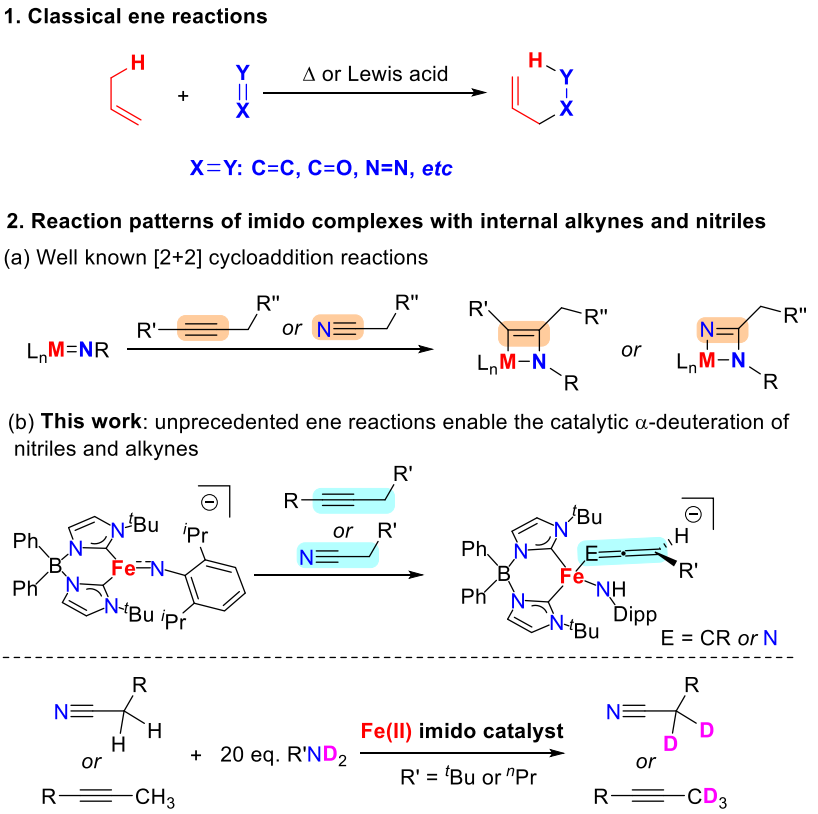


**Scheme 2. Reactions of an Iron(II) Imido Complex with Alkynes and Nitriles**

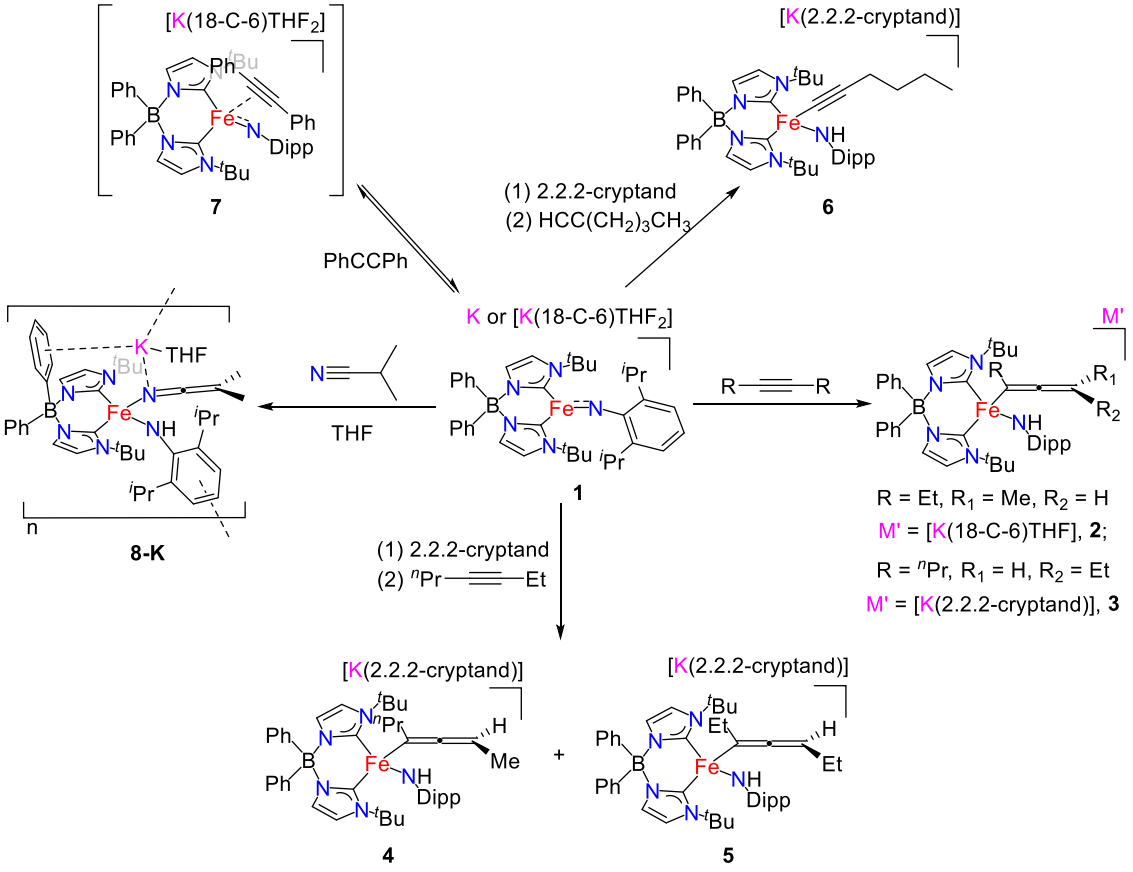




https://doi.org/10.1021/jacs.2c07462
J. Am. Chem. Soc. 2022, 144, 17165−17172

stoichiometric transformations provide a platform for the catalytic $\alpha$-deuteration of nitriles and alkynes by **1**.

## RESULTS AND DISCUSSION

Reaction of brown-red **1**-[**K**(**18-C-6**)] with 1 equiv EtC≡CEt in THF leads to the formation of the yellow high-spin ($S$ = 2) iron(II) complex [$Ph_2B(^tBuIm)_2Fe$(NHDipp)((Et)C═C═C(Me)(H))][K(18-C-6)THF] (**2**), which can be isolated in 95% yield (Scheme 2). Complex **2** was characterized by single-crystal X-ray diffraction, which establishes a tetrahedral Fe(II) amido allenyl complex (Figure 1a). The most notable feature

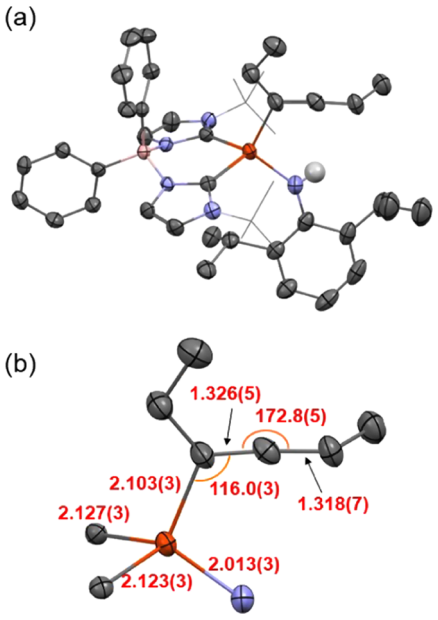


**Figure 1.** Molecular structure of **2** (a), as determined by single-crystal X-ray diffraction. Thermal ellipsoids are shown at a 50% probability level; ligand *tert*-butyl groups are represented as wireframes. Solvent molecules, cations, and most hydrogen atoms are omitted for clarity. The core structure of **2** (b) with selected bond distances (Å) and angles (°). Dark gray, light gray, pink, orange, and blue ellipsoids represent carbon, hydrogen, boron, iron, and nitrogen atoms, respectively.

of the structure is the new allenyl ligand, which is characterized by adjacent C−C double bonds (1.326(5) and 1.318(7) Å) and linear C−C−C (172.8(5)°) linkage (Figure 1b). The Fe−C(allenyl) bond distance in **2** (2.103(3) Å) is in the range observed for $\sigma$ Fe−C(hydrocarbyl) bonds.[37−41] The structure also reveals that the imido ligand in **1**-[**K**(**18-C-6**)] is protonated to provide an amido ligand (Fe−N 2.013(3) Å), with the proton located in the Fourier difference map and refined freely. All other bond metrics are typical for a high-spin ($S$ = 2) iron(II) complex.[41,42]

The allenyl ligand has also been spectroscopically characterized. Specifically, the solution IR spectrum shows a medium intensity band ($\nu_{CCC}$ = 1882 $cm^{-1}$) that is comparable with data for other allenyl complexes.[43,44] In addition, the amido N−H stretch was observed as a sharp band at 3630 $cm^{-1}$ in the solid-state IR spectrum.

As expected for a high-spin complex, the $^1$H NMR spectrum of **2** in THF-$d_8$ shows paramagnetically shifted resonances between −60 and 120 ppm. The solution magnetic moment ($\mu_{eff}$ = 5.3(1) $\mu_B$) is consistent with the high-spin state assignment. This is further supported by zero-field $^{57}$Fe Mössbauer spectroscopy, with spectral parameters ($\delta$ = 0.70 mm/s, $|\Delta E_Q|$ = 3.11 mm/s at 80 K) that are comparable with other tetrahedral $S$ = 2 Fe(II) complexes.[41,42,45]

Similarly, the reaction of **1-K** with 1 equiv $^n$PrC≡C$^n$Pr or $^n$PrC≡CEt in the presence of 2.2.2-cryptand affords the high-spin Fe(II) amido allenyl complexes [$Ph_2B(^tBuIm)_2Fe$(NHDipp)((R$_1$)C═C═C(R$_2$)(H))][K(2.2.2-cryptand)] (R$_1$ = $^n$Pr, R$_2$ = Et, **3**; R$_1$ = $^n$Pr, R$_2$ = Me, **4**; R$_1$ = R$_2$ = Et, **5**) (Scheme 2). The structures of these complexes were also confirmed by single-crystal X-ray diffraction and showed similar structural metrics to **2** (see the SI for details). Interestingly, the reaction of **1-K** with the nonsymmetric alkyne $^n$PrC≡CEt affords two isomers, **4** and **5**, with an occupancy ratio of 1.4:1 according to single-crystal X-ray diffraction. A similar ratio (1.2:1) is observed in solution, as characterized by $^1$H NMR spectroscopy (Figure S9). The preferential formation of **4** is likely determined by steric effects, where $\alpha$-C−H deprotonation on the less hindered ethyl end of $^n$PrC≡CEt is slightly favored.

Complexes **2**−**5** are unique examples of open-shell metal allenyl complexes. While allenyl complexes are typically synthesized by oxidative addition of propargyl halides at low-valent metal centers,[46−50] they can also be accessed through the deprotonation of coordinated alkyne and allene ligands by an external base.[50−52] The synthesis of **2**−**5** is conceptually similar to the latter route, except that the imido ligand acts as an internal base.

In contrast to internal alkynes, the reaction of **1-K** with 1-hexyne in the presence of 2.2.2-crypt and provides the high-spin Fe(II) amido alkynyl complex [$Ph_2B(^tBuIm)_2Fe$(NHDipp)(C≡C(CH$_2$)$_3$CH$_3$)][K(2.2.2-cryptand)] (**6**) which has also been characterized by single-crystal X-ray diffraction (Scheme 2). Similar reactivity with terminal alkynes has been observed for other metal imido complexes.[24,28] The preferential formation of **6** over isomeric allenyl complexes is likely dictated by the greater acidity of the C(sp)−H bond in 1-hexyne.

We also investigated the reactivity of **1**-[**K**(**18-C-6**)] toward diphenylacetylene, which lacks an $\alpha$-C−H group. While no new complexes could be isolated, a new set of resonances is observed in the $^1$H NMR spectrum of an equimolar solution of **1**-[**K**(**18-C-6**)] and PhC≡CPh (Figures S12 and S13). These resonances are tentatively assigned to the $\eta^2$-alkyne imido complex [$Ph_2B(^tBuIm)_2Fe$(NDipp)(PhC≡CPh)][K(18-C-6)THF$_2$] (**7**), which is in equilibrium with **1**-[**K**(**18-C-6**)] and PhC≡CPh in solution ($K_{eq}$ ≈ 0.2 mol/L). This result suggests that the formation of the amido allenyl complexes **2**−**5** is initiated by alkyne coordination to the Fe center, followed by intramolecular proton transfer from the acidic $\alpha$-C−H bond to the basic imido ligand. This proposal is supported by the high basicity of **1**-[**K**(**18-C-6**)], with the estimated p$K_a$(THF) = 42.2 for its conjugate acid, $Ph_2B(^tBuIm)_2Fe$(NHDipp); see the SI for details.

The ene-like reactivity of the Fe(II) imido complex can be extended to nitriles, where the acidic $\alpha$-C−H bond facilitates the formation of keteniminate complexes.[53] For example, the reaction of **1-K** with 1 equiv isobutyronitrile results in the formation of the orange amido keteniminate complex [$Ph_2B(^tBuIm)_2Fe$(NHDipp)(N═C═CMe$_2$)K(THF)]$_n$ (**8-K**) in 87% yield (Scheme 2).[54] Structural characterization of this complex reveals a one-dimensional polymeric chain in which $K^+$ is coordinated to the keteniminate nitrogen atom, a bis(carbene)borate ligand phenyl group and the Dipp group of


https://doi.org/10.1021/jacs.2c07462
J. Am. Chem. Soc. 2022, 144, 17165−17172

a neighboring complex (Figure 2a). The keteniminate ligand is characterized by a linear N−C−C (178.9(3)°) linkage and

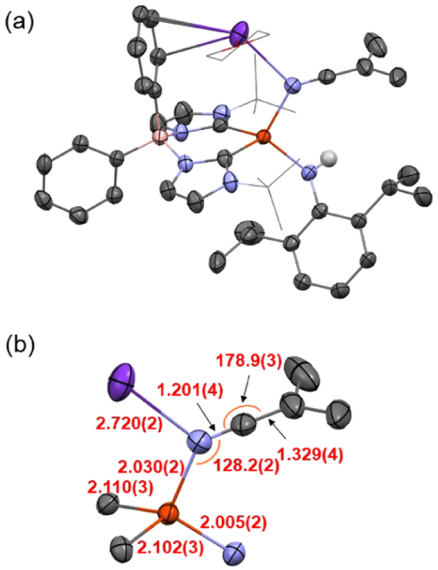


**Figure 2.** Molecular structure of the repeating unit of **8-K** (a), as determined by single-crystal X-ray diffraction. Thermal ellipsoids are shown at a 50% probability level; ligand *tert*-butyl groups and coordinating THF molecule are represented as wireframes. Most hydrogen atoms are omitted for clarity. The core structure of **8-K** (b) with selected bond distances (Å) and angles (°). Dark gray, light gray, pink, orange, blue, and purple ellipsoids represent carbon, hydrogen, boron, iron, nitrogen, and potassium atoms, respectively.

short C-N (1.201(4) Å) and C−C (1.329(4) Å) distances that are consistent with double bonds (Figure 2b). The Fe−N(keteniminate) bond distance (2.030(2) Å) is similar to those observed in high-spin iron(II) amido complexes.[55] Interestingly, the keteniminate Fe−N−C angle (128.2(2)°) shows a large deviation from linearity, in contrast to other keteniminate complexes.[56−60]

This complex has also been spectroscopically characterized. The ketimininate ligand is characterized by absorption in the solution IR spectrum ($\nu_{NCC}$ = 2016 $cm^{-1}$), which is shifted by *ca.* 230 $cm^{-1}$ from isobutyronitrile ($\nu_{NC}$ = 2244 $cm^{-1}$) and is comparable with other metal keteniminate complexes.[58] Unfortunately, we do not observe the amido N−H stretch in either the solid-state or solution IR spectra. The solution magnetic moment (5.0(1) $\mu_B$) in combination with $^{57}$Fe Mössbauer metrics ($\delta$ = 0.67 mm/s and $|\Delta E_Q|$ = 2.94 mm/s at 80 K) confirm the high-spin nature of **8-K**.

The formation of Fe(II) amido allenyl and Fe(II) amido keteniminate complexes can be viewed as ene reactions of the Fe(II) imido complex with internal alkynes and nitriles, respectively. To the best of our knowledge, this type of reaction has never been observed on metal−ligand multiple bonds. We attribute the unusual outcome of these reactions to the combination of strongly basic imido ligand and the coordinately unsaturated Fe center in **1**.

Based on these results, we propose a mechanism for the formation of these complexes (Scheme 3). Alkyne and nitrile coordination to the Fe center affords intermediates **A** and **A′**, respectively. Subsequent internal proton transfer from the alkyne and nitrile ligands to the basic imido is accompanied by

**Scheme 3. Proposed Mechanism for the Formation of the Fe Amido Allenyl and Fe Amido Keteniminate Complexes**

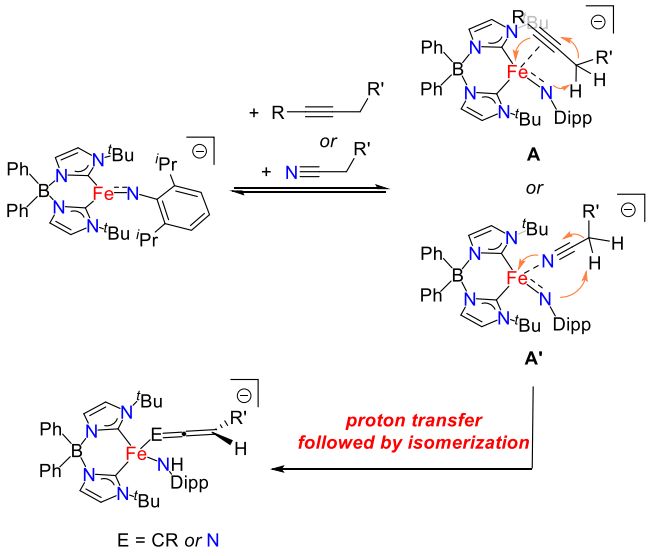


isomerization, yielding the final allenyl and keteniminate products.

DFT calculations were performed to probe the electronic structures of **2** and **8**. Structural optimization provides bond metrics that reproduce those found in the solid-state structures (Tables S1 and S2). Notably, the optimized structure of **8** reveals a bent keteniminate Fe−N−C angle (131.0°), which is similar to that observed in the solid-state structure (128.2(2)°). This bending suggests that the keteniminate ligand is unable to act as a $\pi$-donor to iron, which is expected to increase the basicity of this ligand.

Analysis of the frontier molecular orbitals supports this hypothesis. Specifically, the highest doubly occupied non-metal-based molecular orbitals (HOMO − 5) reveal a significant contribution from the $\beta$-carbon *p*-orbital of the keteniminate ligand in **8** (Figures 3 and S64).[61] Similarly, there is a significant contribution to the corresponding orbital from the $\gamma$-carbon *p*-orbital of the allenyl ligand in **2** (Figures 3 and

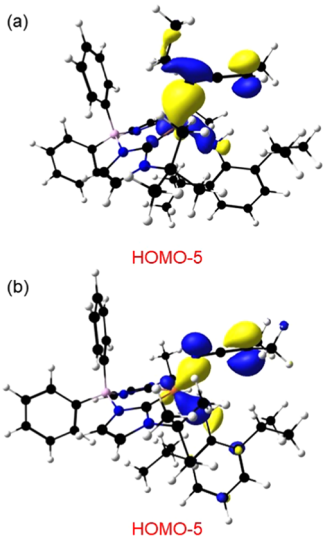


**Figure 3.** Computed HOMO − 5 for **2** (a) and **8** (b). Natural orbitals shown with isodensity = 0.05.



https://doi.org/10.1021/jacs.2c07462
J. Am. Chem. Soc. 2022, 144, 17165−17172

**Scheme 4. Reactions of 2 and 8-K with $RNH_2$ (R = Dipp or $^t$Bu); Catalytic Cycle for the α-Deuteration of Nitriles and Alkynes with $^t$BuND$_2$.**

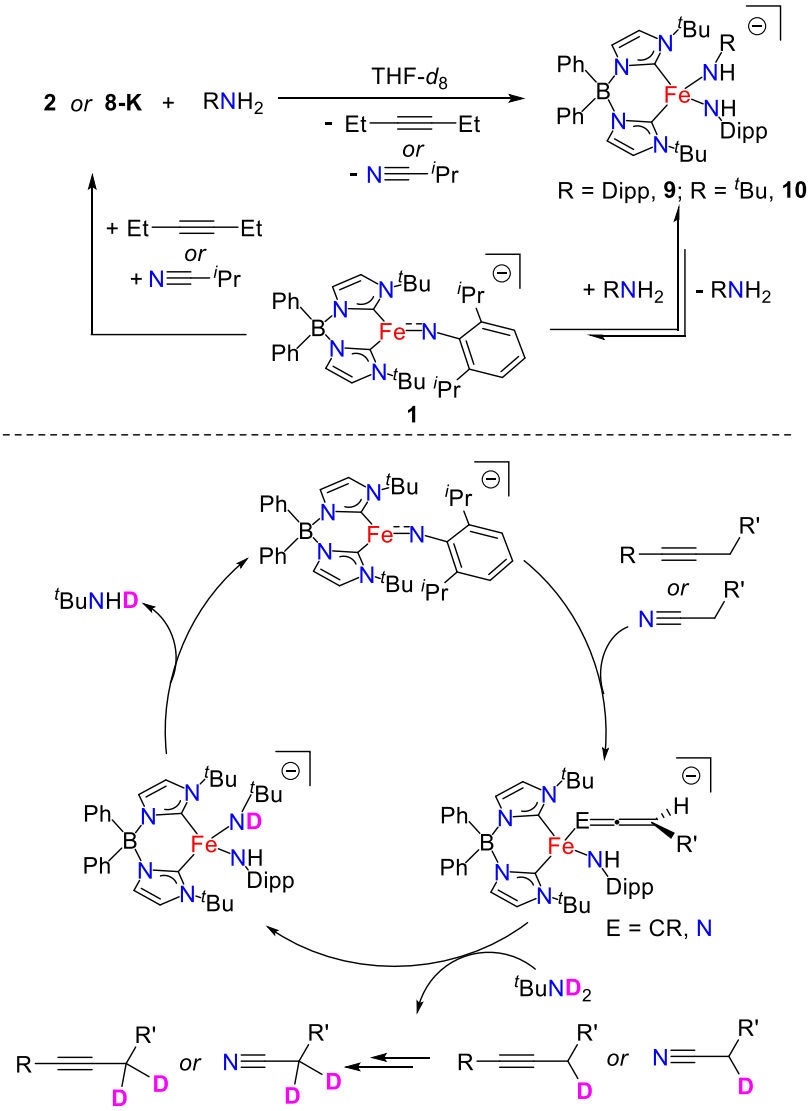


**Table 1. Catalytic α-Deuteration of Nitriles**[a]

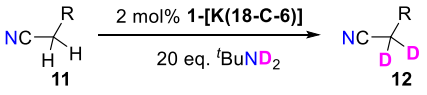


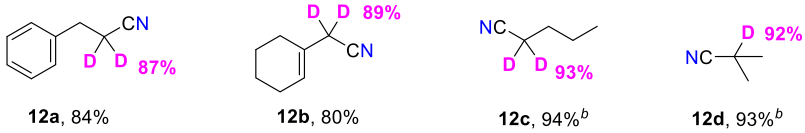


**12a**, 84% **12b**, 80% **12c**, 94%[b] **12d**, 93%[b]

[a]Reaction conditions: 0.5 mol/L nitrile in THF with 20 equiv $^t$BuND$_2$ in the presence of 2 mol % catalyst at room temperature for 12 h, isolated yields reported; [b] NMR yield using mesitylene as the internal standard.

S65). Consequently, the calculated Mulliken atomic charges on these carbon atoms are −0.45 and −0.58 (Figure S66), respectively, suggesting these atoms as the locus of nucleophilic reactivity.[49,51] Confirming these predictions, the reaction of **2** and **8-K** with the weak acid $DippNH_2$ results in the regeneration of 3-hexyne and isobutyronitrile, respectively, along with the formation of the previously reported bis(anilido) complex $[Ph_2B(^t BuIm)_2Fe(NHDipp)_2]^-$ (**9**) (Scheme 4, top).[35] These reactions show no evidence for the formation of free allene and ketenimine. The less acidic amine $^t BuNH_2$ reacts similarly, in this case providing the spectroscopically characterized complex $[Ph_2B(^t BuIm)_2Fe(NH^t Bu)(NHDipp)]^-$ (**10**) (Figures S17 and S18).[62]



https://doi.org/10.1021/jacs.2c07462
J. Am. Chem. Soc. 2022, 144, 17165−17172

Table 2. Catalytic $\alpha$-Deuteration of Alkynes[a]

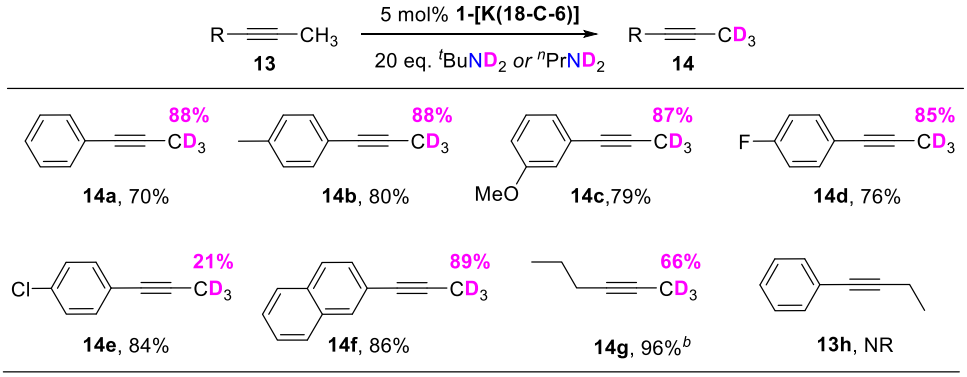


[a]Reaction conditions: 0.5 mol/L alkyne in THF with 20 equiv $^{t}BuND_2$ in the presence of 5 mol % catalyst at 50 °C for 4 d, isolated yields reported; [b] $^{n}PrND_2$ was used with $C_6D_6$ as the solvent, NMR yield using mesitylene as the internal standard.

Complexes **9** and **10** are in equilibrium with **1** and $DippNH_2$ and $^{t}BuNH_2$ in the THF solution, respectively.[35]

Based on these results, we hypothesized that **1** would catalyze the $\alpha$-deuteration of alkynes and nitriles using $^{t}BuND_2$ as the deuterium source (Scheme 4, bottom). In a preliminary demonstration of this reactivity, we observe the $\alpha$-deuteration of a series of aliphatic nitriles in the presence of excess $^{t}BuND_2$ using a 2 mol % **1**-[**K(18-C-6)**] catalyst at room temperature (Table 1).[63] High levels of enrichment are observed, with deuteration being highly selective, as evidenced by the deuteration of 3-phenylpropionitrile, which occurs exclusively at the 1-position.[64] While a small number of metal complexes have been reported to catalyze $\alpha$-deuteration of nitriles,[65,66] the mild conditions for catalysis by **1**-[**K(18-C-6)**] are notable. Heating is required to drive most of the other catalytic nitrile $\alpha$-deuteration reactions.

More interestingly, **1**-[**K(18-C-6)**] is also a catalyst for the selective $\alpha$-deuteration of alkynes (Table 2), albeit with a slightly higher catalyst loading. Deuteration is remarkably selective, exclusively occurring at the terminal methyl group of the alkyne. The lack of activity for $\alpha$-methylene deuteration likely the result of greater steric hindrance at this position. Deuteration is observed for a range of substituted phenylalkynes, although substrates with electron-donating groups are better tolerated in the reaction. Moreover, the selectivity can be controlled through the appropriate amine deuterium source. Thus, while deuteration of phenylalkynes can be achieved using $^{t}BuND_2$, alkyl-substituted alkynes require the less sterically hindered amine $^{n}PrND_2$ for deuteration, likely due to the greater steric constraints of the alkyl chain. To the best of our knowledge, this is the first example of the catalytic $\alpha$-deuteration of alkynes. These compounds are usually accessed by homologation of terminal alkynes under basic conditions.[67]

## CONCLUSIONS

In summary, we have found that the imido ligand in **1** deprotonates coordinated alkynes and nitriles to form the Fe amido allenyl and Fe amido keteniminate complexes, respectively. These are the first ene-like reactions involving metal−ligand multiple bonds. As predicted by DFT, the $\gamma$-carbon of the allenyl ligand and the $\beta$-carbon of the keteniminate ligand can be protonated by primary amines to regenerate the alkynes and nitriles with the concomitant formation of a bis(anilido) complex. This reactivity enables the selective and efficient $\alpha$-deuteration of nitriles and alkynes using **1** as the catalyst. These results suggest that there are avenues beyond nitrene transfer for metal imido complexes in catalysis.

## ASSOCIATED CONTENT

### Supporting Information

The Supporting Information is available free of charge at https://pubs.acs.org/doi/10.1021/jacs.2c07462.

Full experimental details, including synthetic procedures, spectra, computational information, and crystallographic data (PDF)

Optimized structures (XYZ)

### Accession Codes

CCDC 2189799−2189803 contain the supplementary crystallographic data for this paper. These data can be obtained free of charge via www.ccdc.cam.ac.uk/data_request/cif, or by emailing data_request@ccdc.cam.ac.uk, or by contacting The Cambridge Crystallographic Data Centre, 12 Union Road, Cambridge CB2 1EZ, UK; fax: +44 1223 336033.

## AUTHOR INFORMATION

### Corresponding Author

**Jeremy M. Smith** − *Department of Chemistry, Indiana University, Bloomington, Indiana 47405, United States;* orcid.org/0000-0002-3206-4725; Email: smith962@indiana.edu

### Authors

**Yafei Gao** − *Department of Chemistry, Indiana University, Bloomington, Indiana 47405, United States;* orcid.org/0000-0001-7970-8535

**Maren Pink** − *Department of Chemistry, Indiana University, Bloomington, Indiana 47405, United States;* orcid.org/0000-0001-9049-4574

**Veronica Carta** − *Department of Chemistry, Indiana University, Bloomington, Indiana 47405, United States*

Complete contact information is available at: https://pubs.acs.org/10.1021/jacs.2c07462

### Notes

The authors declare no competing financial interest.



https://doi.org/10.1021/jacs.2c07462
J. Am. Chem. Soc. 2022, 144, 17165−17172

## ■ ACKNOWLEDGMENTS

This material is based upon the work supported by the U.S. Department of Energy, Office of Science, Office of Basic Energy Sciences under Award Number DE-SC0019466. We also thank the NSF for the financial support (OMA-1936353). Support for the acquisition of the Bruker Venture D8 diffractometer through the Major Scientific Research Equipment Fund from the President of Indiana University and the Office of the Vice President for Research is gratefully acknowledged.

## ■ REFERENCES

(1) Adam, W.; Krebs, O. The Nitroso Ene Reaction: A Regioselective and Stereoselective Allylic Nitrogen Functionalization of Mechanistic Delight and Synthetic Potential. *Chem. Rev.* **2003**, *103*, 4131−4146.
(2) Alberti, M.; Orfanopoulos, M. Recent Mechanistic Insights in the Singlet Oxygen Ene Reaction. *Synlett* **2010**, *7*, 999−1026.
(3) Zhao, F.; Zhang, S.; Xi, Z. Silyl-substituted 1,3-Butadienes for Diels-Alder Reaction, Ene Reaction and Allylation Reaction. *Chem. Commun.* **2011**, *47*, 4348−4357.
(4) Baidya, M.; Yamamoto, H. Advancements in the Nascent Nitroso-Ene Reaction. *Synthesis* **2013**, *45*, 1931−1938.
(5) Liu, X.; Zheng, K.; Feng, X. Advancements in Catalytic Asymmetric Intermolecular Ene-Type Reactions. *Synthesis* **2014**, *46*, 2241−2257.
(6) Saha, P.; Saikia, A. K. Ene Cyclization Reaction in Heterocycle Synthesis. *Org. Biomol. Chem.* **2018**, *16*, 2820−2840.
(7) Hoffmann, H. M. R. The Ene Reaction. *Angew. Chem., Int. Ed.* **1969**, *8*, 556−577.
(8) Paderes, G. D.; Jorgensen, W. L. Computer-Assisted Mechanistic Evaluation of Organic Reactions. 20. Ene and Retro-Ene Chemistry. *J. Org. Chem.* **1992**, *57*, 1904−1916.
(9) Niu, D.; Hoye, T. R. The Aromatic Ene Reaction. *Nat. Chem.* **2014**, *6*, 34−40.
(10) Snider, B. B. Lewis-Acid-Catalyzed Ene Reactions. *Acc. Chem. Res.* **1980**, *13*, 426−432.
(11) Carlos Dias, L. Chiral Lewis Acid Catalyzed Ene-Reactions. *Curr. Org. Chem.* **2000**, *4*, 305−342.
(12) Cowley, R. E.; Eckert, N. A.; Vaddadi, S.; Figg, T. M.; Cundari, T. R.; Holland, P. L. Selectivity and Mechanism of Hydrogen Atom Transfer by an Isolable Imidoiron(III) Complex. *J. Am. Chem. Soc.* **2011**, *133*, 9796−9811.
(13) King, E. R.; Hennessy, E. T.; Betley, T. A. Catalytic C-H Bond Amination From High-Spin Iron Imido Complexes. *J. Am. Chem. Soc.* **2011**, *133*, 4917−4923.
(14) Laskowski, C. A.; Miller, A. J.; Hillhouse, G. L.; Cundari, T. R. A Two-Coordinate Nickel Imido Complex That Effects C-H Amination. *J. Am. Chem. Soc.* **2011**, *133*, 771−773.
(15) Zhang, L.; Deng, L. C-H Bond Amination by Iron-Imido/Nitrene Species. *Chin. Sci. Bull.* **2012**, *57*, 2352−2360.
(16) Hennessy, E. T.; Betley, T. A. Complex N-Heterocycle Synthesis via Iron-Catalyzed, Direct C−H Bond Amination. *Science* **2013**, *340*, 591−595.
(17) Hennessy, E. T.; Liu, R. Y.; Iovan, D. A.; Duncan, R. A.; Betley, T. A. Iron-Mediated Intermolecular N-Group Transfer Chemistry with Olefinic Substrates. *Chem. Sci.* **2014**, *5*, 1526−1532.
(18) Wang, L.; Hu, L.; Zhang, H.; Chen, H.; Deng, L. Three-Coordinate Iron(IV) Bisimido Complexes with Aminocarbene Ligation: Synthesis, Structure, and Reactivity. *J. Am. Chem. Soc.* **2015**, *137*, 14196−14207.
(19) Iovan, D. A.; Betley, T. A. Characterization of Iron-Imido Species Relevant for N-Group Transfer Chemistry. *J. Am. Chem. Soc.* **2016**, *138*, 1983−1993.
(20) Liu, Y.; Du, J.; Deng, L. Synthesis, Structure, and Reactivity of Low-Spin Cobalt(II) Imido Complexes $[(Me_3P)_3Co(NAr)]$. *Inorg. Chem.* **2017**, *56*, 8278−8286.
(21) Wilding, M. J. T.; Iovan, D. A.; Betley, T. A. High-Spin Iron Imido Complexes Competent for C-H Bond Amination. *J. Am. Chem. Soc.* **2017**, *139*, 12043−12049.
(22) Wilding, M. J. T.; Iovan, D. A.; Wrobel, A. T.; Lukens, J. T.; MacMillan, S. N.; Lancaster, K. M.; Betley, T. A. Direct Comparison of C-H Bond Amination Efficacy through Manipulation of Nitrogen-Valence Centered Redox: Imido versus Iminyl. *J. Am. Chem. Soc.* **2017**, *139*, 14757−14766.
(23) Wang, P.; Deng, L. Recent Advances in Iron-Catalyzed C-H Bond Amination via Iron Imido Intermediate. *Chin. J. Chem.* **2018**, *36*, 1222−1240.
(24) Cheng, J.; Liu, J.; Leng, X.; Lohmiller, T.; Schnegg, A.; Bill, E.; Ye, S.; Deng, L. A Two-Coordinate Iron(II) Imido Complex with NHC Ligation: Synthesis, Characterization, and Its Diversified Reactivity of Nitrene Transfer and C-H Bond Activation. *Inorg. Chem.* **2019**, *58*, 7634−7644.
(25) Cao, C.; Mao, G.; Cheng, J.; Leng, X.; Deng, L. Reactions of a Bis(vinyltrimethylsilane)nickel(0) N-Heterocyclic Carbene Complex with Organic Azides. *J. Organomet. Chem.* **2020**, *913*, 121195−121203.
(26) Coin, G.; Patra, R.; Rana, S.; Biswas, J. P.; Dubourdeaux, P.; Clémancey, M.; de Visser, S. P.; Maiti, D.; Maldivi, P.; Latour, J. M. Fe-Catalyzed Aziridination Is Governed by the Electron Affinity of the Active Imido-Iron Species. *ACS Catal.* **2020**, *10*, 10010−10020.
(27) Kawakita, K.; Kakiuchi, Y.; Tsurugi, H.; Mashima, K.; Parker, B. F.; Arnold, J.; Tonks, I. A. Reactivity of Terminal Imido Complexes of Group 4-6 Metals: Stoichiometric and Catalytic Reactions Involving Cycloaddition with Unsaturated Organic Molecules. *Coord. Chem. Rev.* **2020**, *407*, No. 213118.
(28) Du, J.; Wang, L.; Xie, M.; Deng, L. A Two-Coordinate Cobalt(II) Imido Complex with NHC Ligation: Synthesis, Structure, and Reactivity. *Angew. Chem., Int. Ed.* **2015**, *54*, 12640−12644.
(29) Pugh, S. M.; Trösch, D. J. M.; Wilson, D. J.; Bashall, A.; Cloke, F. G. N.; Gade, L. H.; Hitchcock, P. B.; McPartlin, M.; Nixon, J. F.; Mountford, P. Cycloaddition Reactions of the Titanium Imide $[Ti(NBu^t)\{MeC(2\text{-}C_5H_4N)(CH_2NSiMe_3)_2\}(py)]$ with $Bu^tCP$ and MeCN. *Organometallics* **2000**, *19*, 3205−3210.
(30) Manßen, M.; de Graaff, S.; Meyer, M. F.; Schmidtmann, M.; Beckhaus, R. Direct Access to Titanocene Imides via Bis($\eta^5$:$\eta^1$-pentafulvene)titanium Complexes and Primary Amines. *Organometallics* **2018**, *37*, 4506−4514.
(31) Richards, C. A.; Rath, N. P.; Neely, J. M. Isolation and Reactivity of an Iron Azametallacyclobutene Complex. *Organometallics* **2022**, *41*, 1763−1768.
(32) Baek, Y.; Betley, T. A. Catalytic C−H Amination Mediated by Dipyrrin Cobalt Imidos. *J. Am. Chem. Soc.* **2019**, *141*, 7797−7806.
(33) Baek, Y.; Hennessy, E. T.; Betley, T. A. Direct Manipulation of Metal Imido Geometry: Key Principles to Enhance C−H Amination Efficacy. *J. Am. Chem. Soc.* **2019**, *141*, 16944−16953.
(34) Liu, Q.; Long, L.; Ma, P.; Ma, Y.; Leng, X.; Xiao, J.; Chen, H.; Deng, L. Synthesis, Structure, and C−H Bond Activation Reaction of an Iron(IV) Terminal Imido Complex Bearing Trifluoromethyl Groups. *Cell Rep. Phys. Sci.* **2021**, *2*, No. 100454.
(35) Gao, Y.; Carta, V.; Pink, M.; Smith, J. M. Catalytic Carbodiimide Guanylation by a Nucleophilic, High Spin Iron(II) Imido Complex. *J. Am. Chem. Soc.* **2021**, *143*, 5324−5329.
(36) Gao, Y.; Pink, M.; Smith, J. M. Alkali Metal Ions Dictate the Structure and Reactivity of an Iron(II) Imido Complex. *J. Am. Chem. Soc.* **2022**, *144*, 1786−1794.
(37) Yu, Y.; Sadique, A. Z.; Smith, J. M.; Dugan, T. R.; Cowley, R. E.; Brennessel, W. W.; Flaschenriem, C. J.; Bill, E.; Cundari, T. R.; Holland, P. L. The Reactivity Patterns of Low-Coordinate Iron-Hydride Complexes. *J. Am. Chem. Soc.* **2008**, *130*, 6624−6638.
(38) Liu, Y.; Shi, M.; Deng, L. Iron(II) Dihydrocarbyls Supported by a Biphenyl-Linked Bis(benzimidazol-2-ylidene) Ligand: Syntheses and Characterization. *Organometallics* **2014**, *33*, 5660−5669.
(39) Liu, Y.; Wang, L.; Deng, L. Three-Coordinate Iron(II) Dialkenyl Compound with NHC Ligation: Synthesis, Structure, and Reactivity. *Organometallics* **2015**, *34*, 4401−4407.


https://doi.org/10.1021/jacs.2c07462
J. Am. Chem. Soc. 2022, 144, 17165−17172

(40) Mo, Z.; Deng, L. Open-Shell Iron Hydrocarbyls. *Coord. Chem. Rev.* **2017**, *350*, 285−299.
(41) Lutz, S. A.; Hickey, A. K.; Gao, Y.; Chen, C. H.; Smith, J. M. Two-State Reactivity in Iron-Catalyzed Alkene Isomerization Confers σ-Base Resistance. *J. Am. Chem. Soc.* **2020**, *142*, 15527−15535.
(42) Hickey, A. K.; Lee, W. T.; Chen, C. H.; Pink, M.; Smith, J. M. A Bidentate Carbene Ligand Stabilizes a Low-Coordinate Iron(0) Carbonyl Complex. *Organometallics* **2016**, *35*, 3069−3073.
(43) Coletti, C.; Gonsalvi, L.; Guerriero, A.; Marvelli, L.; Peruzzini, M.; Reginato, G.; Re, N. Electron-Poor Rhenium Allenylidenes and Their Reactivity toward Phosphines: A Combined Experimental and Theoretical Study. *Organometallics* **2012**, *31*, 57−69.
(44) Johnson, A.; Laguna, A.; Gimeno, M. C. Axially Chiral Allenyl Gold Complexes. *J. Am. Chem. Soc.* **2014**, *136*, 12812−12815.
(45) Liu, Y.; Luo, L.; Xiao, J.; Wang, L.; Song, Y.; Qu, J.; Luo, Y.; Deng, L. Four-Coordinate Iron(II) Diaryl Compounds with Monodentate N-Heterocyclic Carbene Ligation: Synthesis, Characterization, and Their Tetrahedral-Square Planar Isomerization in Solution. *Inorg. Chem.* **2015**, *54*, 4752−4760.
(46) Canovese, L.; Visentin, F.; Biz, C.; Scattolin, T.; Santo, C.; Bertolasi, V. Oxidative Addition of Allyl and Propargyl Halides on Palladium(0) Complexes Bearing Bidentate Ligands with Quinolinic Structure. *J. Organomet. Chem.* **2015**, *786*, 21−30.
(47) Hoseini, S. J.; Fath, R. H.; Hashemian, F.; Rashidi, M. Oxidative Addition Reaction of Allyl or Propargyl Bromide with a Diarylplatinum(II) Complex. *J. Organomet. Chem.* **2016**, *822*, 5−12.
(48) Canovese, L.; Scattolin, T.; Visentin, F.; Santo, C. Reactions of Palladium(0) Olefin Complexes Stabilized by Some Different Hetero- and Homo-ditopic Spectator Ligands with Propargyl Halides. *J. Organomet. Chem.* **2017**, *834*, 10−21.
(49) Fernández, S.; Gonzalez, J.; Santamaria, J.; Ballesteros, A. Propargylsilanes as Reagents for Synergistic Gold(I)-Catalyzed Propargylation of Carbonyl Compounds: Isolation and Characterization of σ-Gold(I) Allenyl Intermediates. *Angew. Chem., Int. Ed.* **2019**, *58*, 10703−10707.
(50) Wojcicki, A. Allenyls and Propargyls: Versatile Ligands in Transition-Metal Chemistry. *Inorg. Chem. Commun.* **2002**, *5*, 82−97.
(51) Wang, Y.; Zhu, J.; Durham, A. C.; Lindberg, H.; Wang, Y. M. α-C-H Functionalization of π-Bonds Using Iron Complexes: Catalytic Hydroxyalkylation of Alkynes and Alkenes. *J. Am. Chem. Soc.* **2019**, *141*, 19594−19599.
(52) Wang, Y.; Durham, A. C.; Wang, Y. Redox-Neutral Propargylic C−H Functionalization by Using Iron Catalysis. *Synlett* **2020**, *31*, 1747−1752.
(53) Zhao, J.; Zhang, S.; Zhang, W. X.; Xi, Z. Formation of Zirconocenes Containing Vinyl-imine and Keteniminate Species from Zirconacycles and Diphenylacetonitrile. *Organometallics* **2011**, *30*, 3464−3467.
(54) Similar reactivity is observed with **1**-[**K**(**18-C-6**)], however the resulting keteniminate product is significantly less stable, suggesting that $K^+$ coordination plays a key role in stabilizing **8**.
(55) Wang, X.; Mo, Z.; Xiao, J.; Deng, L. Monomeric Bis(anilido)-iron(II) Complexes with N-Heterocyclic Carbene Ligation: Synthesis, Characterization, and Redox Reactivity Toward Aryl Halides. *Inorg. Chem.* **2013**, *52*, 59−65.
(56) Fedushkin, I. L.; Morozov, A. G.; Chudakova, V. A.; Fukin, G. K.; Cherkasov, V. K. Magnesium(II) Complexes of the dpp-BIAN Radical-Anion: Synthesis, Molecular Structure, and Catalytic Activity in Lactide Polymerization. *Eur. J. Inorg. Chem.* **2009**, *2009*, 4995−5003.
(57) Zhao, J.; Zhang, S.; Zhang, W. X.; Xi, Z. Reactivity of Seven-Membered Azazirconacycloallenes and Four-Membered Zirconacycles toward Diphenylacetonitrile. *Organometallics* **2012**, *31*, 8370−8374.
(58) Becker, L.; Burlakov, V. V.; Arndt, P.; Spannenberg, A.; Baumann, W.; Jiao, H.; Rosenthal, U. Reactions of Group 4 Metallocene Complexes with Mono- and Diphenylacetonitrile: Formation of Unusual Four- and Six-Membered Metallacycles. *Chem. - Eur. J.* **2013**, *19*, 4230−4237.
(59) Becker, L.; Haehnel, M.; Spannenberg, A.; Arndt, P.; Rosenthal, U. Reactions of Group 4 Metallocenes with Monosubstituted Acetonitriles: Keteniminate Formation versus C-C Coupling. *Chem. - Eur. J.* **2015**, *21*, 3242−3248.
(60) Hale, L. V. A.; Sikes, N. M.; Szymczak, N. K. Reductive C-C Coupling from α,β-Unsaturated Nitriles by Intercepting Ketenimines. *Angew. Chem., Int. Ed.* **2019**, *58*, 8531−8535.
(61) The highest energy occupied molecular orbitals are all metal based, see Figures S64 and S65.
(62) Heat is required to drive the reaction of **2** with $^t$BuNH$_2$. The formation of 3-hexyne is observed by $^1$H NMR, however the formation of multiple products occurs, likely due to the decomposition of **10** under the thermal condition.
(63) We find that the analogous deuteration of phenylpropionitrile and its derivatives by $^t$BuND$_2$ occurs without the need for a catalyst.
(64) The estimated KIE for the nitrile substrates is $k_H/k_D \approx 3$ based on the initial rates for the catalytic deuteration of PhCH$_2$CH$_2$CN and the protiation of PhCH$_2$CD$_2$CN with 10 eq. $^t$BuND$_2$ and $^t$BuNH$_2$, respectively (2 mol% iron imido catalyst).
(65) Krishnakumar, V.; Gunanathan, C. Ruthenium-Catalyzed Selective α-Deuteration of Aliphatic Nitriles Using D$_2$O. *Chem. Commun.* **2018**, *54*, 8705−8708.
(66) Zhou, Q. Q.; Zou, Y. Q.; Kar, S.; Diskin-Posner, Y.; Ben-David, Y.; Milstein, D. Manganese-Pincer-Catalyzed Nitrile Hydration, α-Deuteration, and α-Deuterated Amide Formation via Metal Ligand Cooperation. *ACS Catal.* **2021**, *11*, 10239−10245.
(67) Davison, R. T.; Parker, P. D.; Hou, X.; Chung, C. P.; Augustine, S. A.; Dong, V. M. Enantioselective Addition of α-Nitroesters to Alkynes. *Angew. Chem., Int. Ed.* **2021**, *60*, 4599−4603.




https://doi.org/10.1021/jacs.2c07462
J. Am. Chem. Soc. 2022, 144, 17165−17172